

Preparing ITER ICRF: Test of the Load Resilient Matching Systems on an Antenna Mock-up

P. Dumortier, F. Durodié, D. Grine, R. Koch, P.U. Lamalle¹, F. Louche, A. Messiaen, M. Vervier, R. Weynants

Laboratory for Plasma Physics, Association EURATOM - Belgian State, partner in the Trilateral Euregio Cluster, Royal Military Academy, 30 av. de la Renaissance, B-1000 Brussels, Belgium

e-mail contact of main author: a.messiaen@fz-juelich.de

Abstract. The reference design for the ICRF antenna of ITER is constituted by a tight array of 24 straps grouped in 8 triplets. The matching network must be load resilient for operation in ELMy discharges and must have wave spectrum control for heating or current drive operation. The load resilience is based on the use of either hybrid couplers or Conjugate-T circuits. However the mutual coupling between the triplets at the low expected loading strongly counteracts the load resilience and wave spectrum control. Using a mock-up of the ITER antenna array with adjustable water load matching solutions are designed and tested. We show that suitable decoupler circuits neutralize the mutual coupling effects and that the wave spectrum can be controlled by the anti-node voltage distribution. A matching solution using four 3dB hybrids and the wave spectrum feedback control by the decouplers provides outstanding performances if each pair of poloidal triplets undergoes a same load variation. The Conjugate-T solution is presently considered as a back-up option.

1. Introduction

ITER ICRH system. The ICRF system of ITER must couple 20MW to the plasma in the 40-55MHz frequency band through a surface of $\sim 1.5 \times 1.9 \text{m}^2$, with a wave spectrum appropriate for both heating and current drive. Its matching system must furthermore be resilient to the large load variations that are typical for ELMy discharges. A conceptual design of the ICRH antenna has been developed in 2003 [1] consisting of an array of 24 radiating straps in order to provide the required large power density at an affordable antenna voltage. The 24 straps are combined in 8 triplets by using passive 4-port junctions, thus providing a more uniform RF current distribution among the straps and a reduced maximum strap voltage. It also reduces to 8 the number of feeding lines. No in-vessel remotely operated matching components are foreseen. This overall antenna RF concept has been selected in April 2007 as reference design for the ITER ICRH system [2]. The detailed design that warrants the RF performance, the cooling and neutron shielding requirements as well as the mechanical constraints for strength, fabrication and maintenance is presently in progress [3]. An ICRH antenna array of the projected complexity has not been constructed before. It is of utmost importance to study the critical issues of load resilience and of robustness and reliability of the matching procedure experimentally before the procurement of the ICRH system. In this paper we describe the development hitherto achieved to this end by means of a dedicated mock-up.

Mock-up and plasma loading simulation. The mock-up of the complete antenna array [4] has been constructed starting from the CATIA 3-D drawings of the 2003 design. This design already incorporates all the electrical characteristics of the present detailed one: use of eight 4-port junctions to feed the 24 straps, each strap being in its own antenna box to reduce their mutual coupling, use of same line characteristic impedance (see FIG. 1). A full-scale model is not needed to establish the antenna characteristics: when decreasing the length and increasing the frequency by the same scale factor the impedance matrix of the array remains identical (except for skin losses) in presence of non-dispersive medium. The front face of the mock-up is mounted with sliding contacts through a metal plate simulating the ITER wall. A realistic

¹ New address: ITER Cadarache Joint Work Site, F-13108, St Paul lez Durance, France.

simulation of plasma-like load conditions is obtained [5,6] by facing the strap array by a large dielectric constant medium like water. Load variations are achieved by adjusting the distance water tank-antenna and their effect on the diagonal terms and on the off-diagonal ones (due to mutual coupling between the triplets) of the impedance matrix can be measured. The range of load variation obtained with water load corresponds well to the range predicted for plasma loading with typical SOL decay lengths.

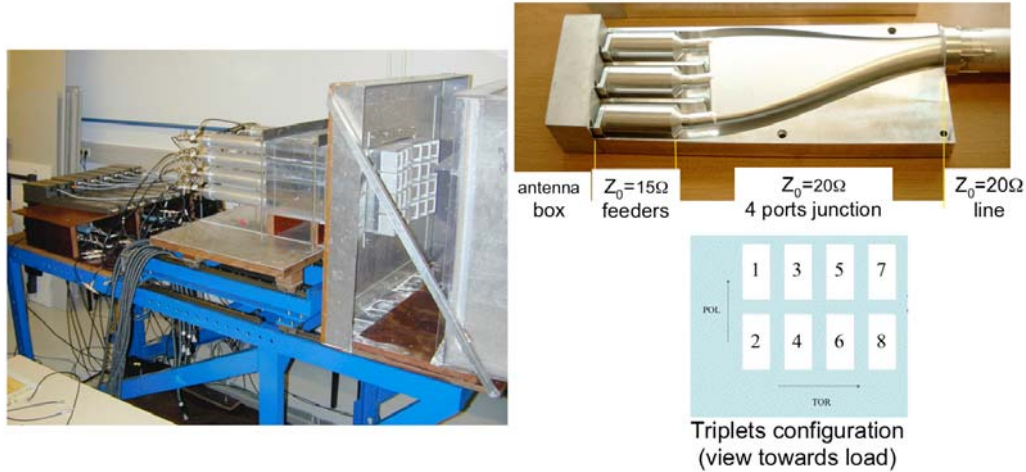


FIG.1a). Mock-up (scale 1/5) with automatic matching system (the water load is removed to show the strap array, the poloidal direction is the horizontal one). 1b). One triplet of straps fed by the 4-port junction and triplet configuration.

2. Selection of load resilient matching layout

The matching procedure must provide real time matching on the reference load, resilience to fast load variations with respect to this reference load and good control of the antenna current spectrum. Furthermore it must provide a robust feedback control of the matching using simple diagnostics. Two challenges have to be faced hereby: (i) Due to the compactness of the array the mutual coupling effects between the radiating triplets are important and lead to a coupling between all matching actuators and power sources, to an asymmetry in the radiated power distribution among the triplets and load resilience degradation. (ii) The low range of antenna loading resistance to be expected in ITER because of the large antenna-plasma separatrix distance renders the adjustment of the matching circuits very critical and intensifies the mutual coupling effects. This leads also to large voltages and currents in the system for radiating the requested nominal power.

To overcome the mutual coupling effects we have successfully tested two methods on the mock-up: (i) the passive power distribution for which pairs of triplets are connected in parallel near a voltage anti-node by T junction [7,8]. This method has the drawbacks to combine the power of several generators in one very high power feeding line and to need line layout modifications for different toroidal phasings. (ii) The use of appropriate decoupler circuits to sufficiently reduce the effect of the reactive part of the mutual coupling terms in the admittance matrix seen by the matching network. In addition the decouplers can also control the antenna current distribution. A decoupler is constituted by 2 sections of $\sim\lambda/4$ lines connected to an adjustable capacitor (see e.g. FIG. 7).

To alleviate the expected low loading by the plasma in ITER two approaches are pursued: (i) The geometry of the antenna box, the 4-port junction and service stub [9] are optimized by modeling and testing on a dedicated mock-up. (ii) A pre-matching is provided by the antenna plug layout and characteristic impedance transition reducing the VSWR at the input of the matching circuit by a factor 6.5 to 11 in the frequency band with appropriate service stub [9].

Two load resilient matching networks are considered: (i) the ‘‘Conjugate-T’’ (CT) circuit which maintains the amount of radiated power during the load variation and (ii) the hybrid coupler which dumps the reflected power into a dummy load. For both networks the load resilience relies on the symmetry of load variations seen by two different antenna triplets. The CT circuit is only resilient to variations of the active part of the loading and is presently considered by ITER as a back-up option, the reference circuit being based on hybrid couplers. The paper describes our present status in the development and testing of a matching system using (i) four CT’s and (ii) four 3dB hybrid junctions.

Our investigation starts with the measurement of the 8x8 scattering matrix of the 8 triplets versus loading conditions at output of the 4-port junctions [4]. Then the 8X8 or 4X4 S, Z or Y matrices are computed and can be checked at any positioning of the matching network and back to the straps [10]. Then the two selected matching network are optimised from modelling and subsequently tested experimentally (as shown in FIG. 1).

3. Study of the 4 ‘‘Conjugate-T’’ (CT) load resilient solution

Layout. The matching network layout is shown in FIG.2. Starting from the output of the antenna plug one finds: (i) the 20Ω line stretchers to preset the locations A...H at voltage anti-node for the operating frequency, (ii) At these locations are connected (a) the 6 toroidal decouplers which are preset with vacuum loading to cancel the reactive part of the mutual admittances with the neighbour triplets, (b) the 50Ω poloidal CT circuit and (c) the feedback controlled stub, (iii) a λ/4 transformer to decrease the VSWR in the 4 long lines connected to the preset second matching stages and (iv) the power sources with feedback control of their phasing and preset of their output forward power.

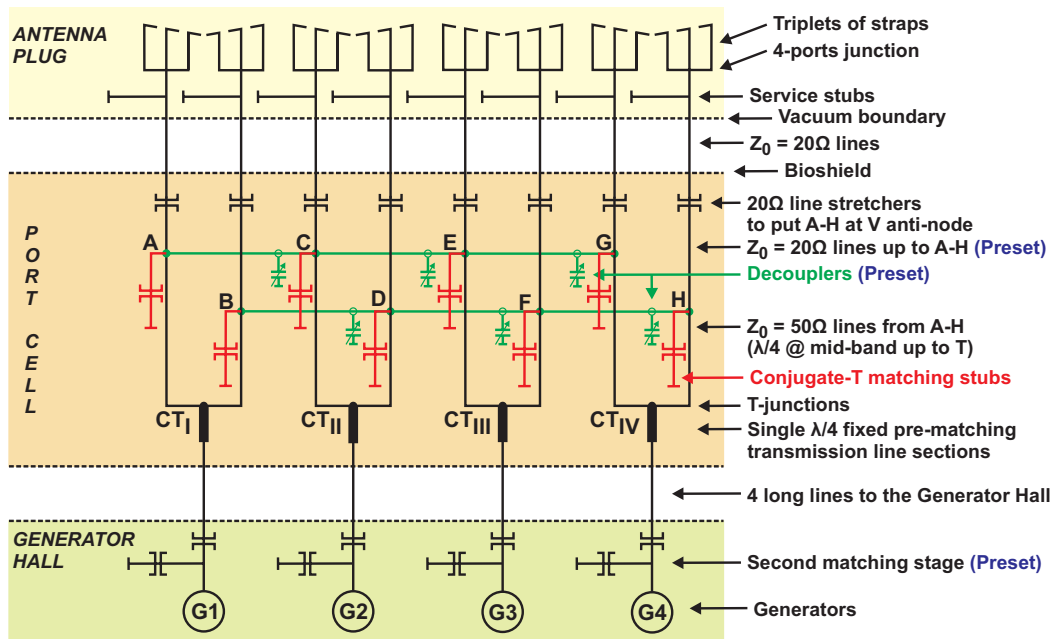


FIG. 2. Layout of the 4 CT matching system with its proposed implementation in ITER.

Strap current distribution and load resilience control. The strap input current I_A being at current anti-node it is very well correlated in amplitude and phase with the corresponding anti-node voltages $V_{A...H}$ in locations A...H. Starting from the measured matrix, the CT matching stubs settings are computed to obtain the desired toroidal and poloidal phasing of I_{Ai} by controlling the $V_{A...H}$ distribution [10,11]. This is done for a chosen reference load. This settles (i) the CT impedances Z_{CT} seen from the generators side and (ii) the ratio of the forward power of the generators. The practical procedure is as follows: the second stage is

preset to match the reference Z_{CT} 's to the generators, the generators forward power is also preset. The CT matching stubs for matching the generators to the reference load and the generator phasing for maintaining the requested toroidal phasing are feedback controlled in real time.

Performances of the matching network. The effective mean antenna resistance $R_{Aeff} = \sum_i (2P_{ari}/|I_{ai}|^2)/(8l_{strap})$ is used to measure the loading (P_{ari} is the active power coupled to strap i , I_{ai} the strap i input current and l_{strap} the strap length). FIG. 3 shows the load resilience obtained for R_{Aeff} larger than the reference $R_{Aeff} = 2\Omega/m$ and the strap current distribution control obtained for the case of toroidal current drive phasing ($0 \pi/2 \pi 3\pi/2$). Almost the total generator power is then radiated. Note that the CT circuit passively modifies the relative phase between the poloidal pair of triplets for obtaining the load resilience. The anti-node voltage is linked to the corresponding strap current amplitude by $|V_{A...H}| \cong 26|I_{ai}|$ (V, A) and the mean conductance at this location $\langle G_{minA...H} \rangle \cong 0.00115 R_{Aeff}$ (S, Ω/m). The VSWR in the 4 long lines to the second matching stages remains lower than 2 for $R_{Aeff} \geq 2\Omega/m$. The experimental set-up successfully testing the simultaneous feedback control of the CT stubs and of the toroidal phasing is shown in FIG. 1. Similar results are obtained with the various heating toroidal phasings. The load resilience gets poorer when the reference R_{Aeff} decreases.

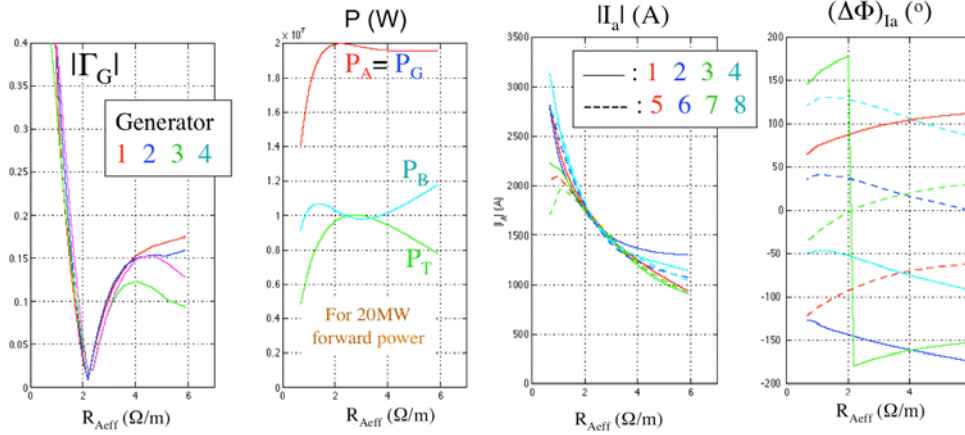


FIG. 3. Reflection coefficient of the 4 generators, total active power delivered by the 4 generators (P_G) equal to the radiated power ($P_A = P_B + P_T$, P_B and P_T in the bottom and top triplets) and mean strap current distribution (amplitude and phase) in the 8 triplets as a function of R_{Aeff} . (Case of CD phasing with reference $R_{Aeff} = 2\Omega/m$, generators forward power: $P_{G+} = 6.2, 4.9, 4.6, 4.2$ MW, $f_{ITER} = 42$ MHz).

4. Study of the 4 hybrid load resilient option

Layout. The matching network is shown in FIG. 4. Starting from the output of the antenna plug one finds: (i) the 20Ω line stretchers to preset the locations A...H at voltage anti-node for the operating frequency, (ii) At these locations are connected (a) the 10 feedback controlled toroidal and poloidal decouplers to reduce the mutual coupling and control the antenna current spectrum and (b) the 50Ω double stub tuners (the first stub being implemented by a capacitor), (iii) the 8 long lines connected to the 3dB quadrature hybrids and (iv) the dummy loads and power sources connected to the remaining ports of the hybrids. Each hybrid is feeding a poloidal pair of triplets.

Load resilience condition. If S_{hyb} is the scattering matrix seen by ports 1 and 4 of the hybrids we have: $E_{Hyb-} = S_{Hyb} E_{Hyb+}$ with $V_{Hyb} = E_{Hyb+} + E_{Hyb-}$ and $E_{Hyb-}/E_{Hyb+} = \Gamma_{Hyb}$ where Γ_{Hyb} is the reflection coefficient vector. We note $\Gamma_1 = \Gamma_{Hyb}(i)$ and $\Gamma_4 = \Gamma_{Hyb}(j)$ the reflection coefficients seen at output 1 and 4 of the hybrids (see FIG. 4). Then the reflection coefficient seen by the power source is $\Gamma_3 = (\Gamma_1 - \Gamma_4)/2$ and the transfer coefficient to the load $S_{LG} = E_2/E_{3+} = (\Gamma_1 + \Gamma_4)/2$. Complete power

dump in the load by the hybrid requires $\Gamma_1 = \Gamma_4$ in amplitude and phase. If the same load variation is seen by the poloidal triplet pair fed by a particular hybrid the condition $\Gamma_1 = \Gamma_4$ is fulfilled if there is complete symmetry of the lines and tuners. This requires a sufficiently low mutual coupling. High mutual coupling will completely inhibit the load resilience of the circuit [12]. The forward voltages in ports 1 and 4 are in quadrature and the forward powers $P_{\text{Hyb}+1}$ and $P_{\text{Hyb}+4}$ are both equal to half the source power P_G .

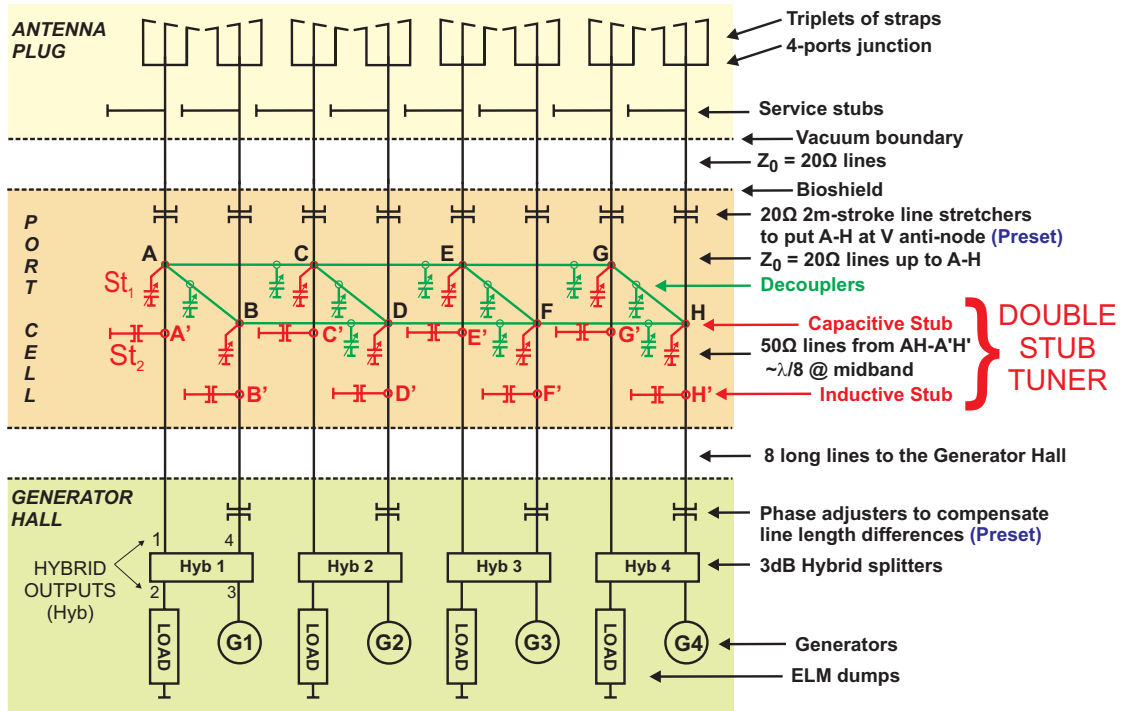


FIG. 4. Layout of the 4 hybrids matching system with its proposed implementation in ITER.

Performances of the matching network. FIG. 5 shows the excellent load resilience and strap current distribution control obtained for the case of toroidal current drive phasing. The system is matched on a reference $R_{\text{Aeff}} = 2\Omega/\text{m}$ for which the total forward power of the generators is delivered to this load. When R_{Aeff} changes the reflected power is dumped in the hybrid dummy loads. Note the equal power delivered to the top and bottom triplets and the

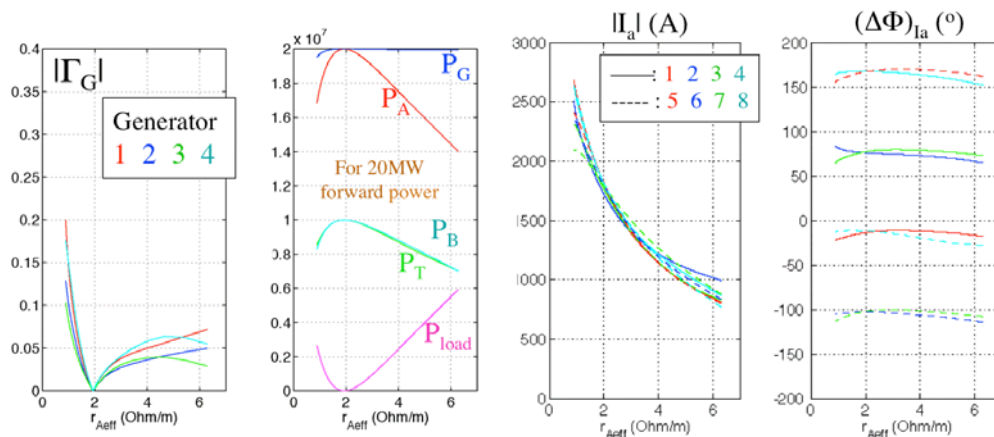


Fig. 5. Reflection coefficient of the 4 generators, active power delivered by the 4 generators (P_G) and its repartition in the radiated power ($P_A = P_B + P_T$) in the top and bottom triplets, power dumped in the load P_{load} , and mean strap current distribution (amplitude and phase) in the 8 triplets as a function of R_{Aeff} . (case of CD phasing with reference $R_{\text{Aeff}} = 2\Omega/\text{m}$, all generators: $P_{G+} = 5\text{MW}$, $f_{\text{ITER}} = 42\text{MHz}$, $|V_{A\dots H}| \cong 26|I_{ai}|$ (V, A), $\langle G_{\text{min}A\dots H} \rangle \cong 0.00115 R_{\text{Aeff}}$ (S, Ω/m)).

nearly equal amplitude of the mean strap current amplitudes of the 8 triplets for the whole range of R_{Aeff} . The relative phase between the triplets is also nearly constant: $\pi/2$ poloidally imposed by the hybrids, and $0 \pi/2 \pi 3\pi/2$ toroidally imposed by a preset phase difference between power sources (no feedback control is necessary as for the CT case).

In FIG. 5 the variation of strap inductance with R_{Aeff} is the one measured on the mock-up. A larger inductance variation during the ELM's is considered by taking the complete antenna Z-matrix $Z_{A0}=R_{A0}+iX_{A0}$ corresponding to the reference $R_{Aeff}=2\Omega/m$ and describing the ELM effect by $Z_A=R_{A0}(1+\Lambda)+i(1-\Lambda/20)X_{A0}$, with $-0.5<\Lambda<4$ (-0.5 is taken to display below

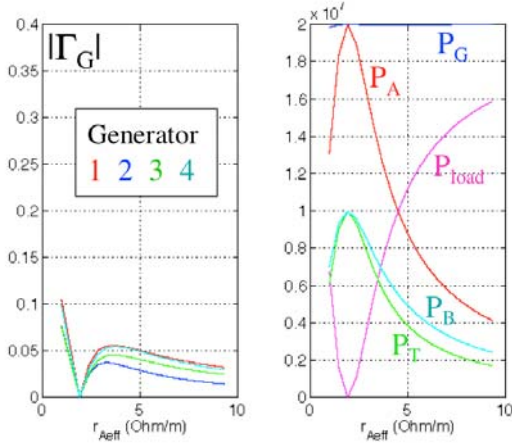


Fig 6. Same as Fig. 5 but with simulation of ELM's effect with large decrease of antenna inductance.

$R_{Aeff}=2\Omega/m$). The corresponding results are shown in FIG. 6. They indicate still excellent load resilience but a larger fraction of the forward power dumped in the loads. In the long lines the VSWR increases up to 18 at the maximum of the ELM perturbation ($\Lambda=4$) and the peak voltage in the long lines up to twice the voltage in matched condition ($R_{Aeff}=2\Omega/m$). These results are obtained with the same forward power of the generators ($P_{G+}=5MW$). If a heating toroidal phasing is chosen ($0\pi 0\pi, 00\pi\pi$ or $0\pi\pi 0$) the same excellent load resilience is observed. The optimal current distribution control requires an additional feedback on the generator power as explained below.

Feedback control of current distribution by the decouplers. If $Y=G+iB$ is the admittance matrix of the 8 lines at some position (from the 4-ports junctions up to the hybrids), the active power $Re(P_j)=Re(V_j I_j^*/2)$ in line j is given by

$$Re(P_j)=0.5[G_{jj}|V_j|^2+\sum_{i\neq j}|V_i||V_j|\{G_{ji}\cos(\Delta\Phi_{ji})+B_{ji}\sin(\Delta\Phi_{ji})\}]\equiv P_{G,ii}+\sum_{i\neq j}P_{G,ji}+\sum_{i\neq j}P_{B,ji} \quad (1)$$

where $V_i=|V_i|\exp(i\Phi_i)$ is the voltage on line i and $\Delta\Phi_{ji}=\Phi_j-\Phi_i$. The contribution $\sum_{i\neq j}P_{G,ji}$ due to the coupling between triplets j and i vanishes when $\Delta\Phi_{ji}=(2n+1)\pi/2$ whereas the contribution $\sum_{i\neq j}P_{B,ji}$ vanishes when $\Delta\Phi_{ji}=n\pi$. If Y is symmetric this last contribution linked to the reactive part of Y corresponds to the sum of exchanged power $P_{B,ji}$ between the triplet j and the 7 other

triplets. Then we have also $P_{B,ji}=-P_{B,ij}$.

For the poloidally adjacent triplets pair fed by each hybrid ($\Delta\Phi_{ji}\equiv\pm\pi/2$) we have $\sum_{i\neq j}P_{B,ji}\neq 0$ in presence of mutual coupling and no $\sum_{i\neq j}P_{G,ji}$ contribution. This is also the case for toroidal adjacent triplets in the case of current drive phasing ($\Delta\Phi_{ji}\equiv\pm\pi/2$).

In the case of heating phasing ($\Delta\Phi_{ji}\equiv\pm\pi$) there is no $\sum_{i\neq j}P_{B,ji}$ contribution between the toroidal adjacent triplets but well a $\sum_{i\neq j}P_{G,ji}$ one.

The circuit connecting a decoupler to two outputs of hybrid (location Hyb) through tuners and to two 20Ω lines coming from the antenna plug at voltage anti-node location T (which stands for A...H) is

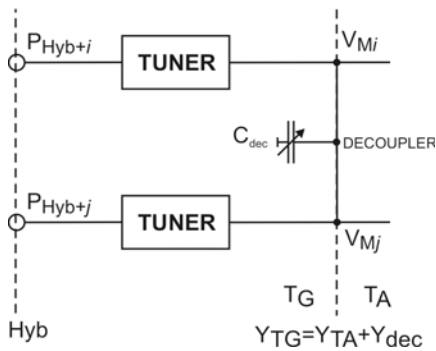


Fig. 7. Connection circuit of one decoupler between lines i and j .

shown in FIG.7. T_A and T_G mean respectively antenna or generator side at location T. The V_{Mi} are the anti-node voltages. If lines i and j are matched the forward active power in Hyb is:

$$P_{Hyb+}=Re(P_{TG})=0.5\{G_{TGjj}|V_{Mj}|^2+\sum_{i\neq j}|V_{Mi}||V_{Mj}|\{G_{TGji}\cos(\Delta\Phi_{Mji})+B_{TGji}\sin(\Delta\Phi_{Mji})\}\} \quad (2)$$

In section 3 we have seen that the antenna current distribution is strongly correlated with the anti-node voltage V_M distribution (in amplitude and phase). Therefore it is sufficient to feedback control this voltage in order to have the same anti-node voltage amplitude $V_{M_i}=V_{M_j}$ for $\text{Re}(P_{\text{Hyb}+i}) = \text{Re}(P_{\text{Hyb}+j})$. The toroidal phasing is imposed by the power sources phasing.

1. *Case of current drive phasing ($\Delta\Phi_{Mji}=(2n+1)\pi/2$)*: The difference $|V_{M_i}|-|V_{M_j}|$ is used as error signal to adjust the decoupler capacitors and therefore $B_{\text{TG}ji}=B_{\text{TA}ji}+ B_{\text{dec},ji}$ with equal forward power of the 4 sources to the 3dB couplers. This procedure just allows the (low) level of $P_{B,ji}$ necessary to maintain the equality of the voltages and strap currents when $G_{\text{TG}ii}\neq G_{\text{TG}jj}$. For the complete system the 10 decouplers maintain the eight V_{M_i} equal in amplitude with the same values of all $\text{Re}(P_{\text{Hyb}+j})$. FIG. 8 illustrates the action of the decouplers to maintain equal active forward power in the 8 lines from the hybrids to the decouplers, although the active power between the decouplers and the triplets is not equal at all and can even reverse at low R_{Aeff} . It shows also that a small amount of exchanged power $\sum_{i\neq j} P_{B,ji}$ among the heating lines is remaining on the generator side of the decouplers to ensure the V_M and $|I_A|$ control. The feedback algorithm is, e.g. for the case of the line connected in A and B to the first triplet, simply $\Delta C_{\text{dec},AB} \propto (|V_A|-|V_B|)$.

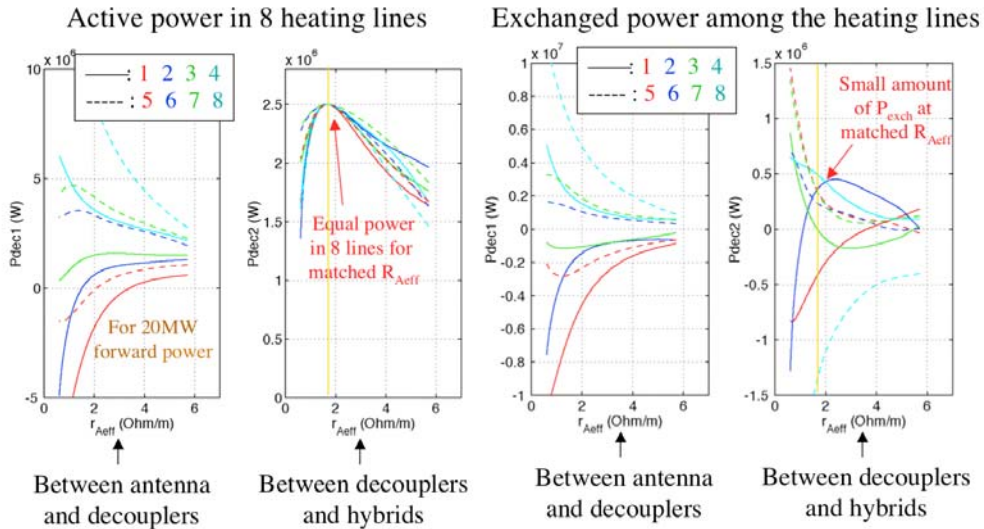


FIG. 8. Power distribution among the 8 triplet feeding lines before and after the decouplers.

2. *Case of heating phasing ($\Delta\Phi_{Mji} = n\pi$ for the toroidal decouplers, $\Delta\Phi_{ji} \approx \pm\pi/2$ for the poloidal decouplers)*: The 4 poloidal decouplers are driven by their voltage amplitude difference $|V_{M_i}|-|V_{M_j}|$ as explained above and maintain equal voltage in each poloidal triplet pair. The toroidal decouplers have no significant influence on the voltage difference between the toroidal pairs. The power source forward power $P_{G+}=2 P_{\text{Hyb}+}$ is therefore used to cancel this voltage amplitude difference. The following difference of anti-node voltage amplitude in A...H is used as error signal: mean value of the two voltages related to a particular hybrid less mean value of the 8 voltages; e.g. for the case of the power source 1 connected to the two first triplets we have: $\Delta P_{G1+} \propto \{(|V_A|+|V_B|)/2 - \langle |V_X| \rangle\}$ with $\langle |V_X| \rangle = \{|V_A|+|V_B|+\dots+|V_H|\}/8$. This control is only necessary if the dissymmetry in the $G_{\text{TG}ij}|V_{M_j}|^2 \pm \sum_{i\neq j} |V_{M_i}||V_{M_j}|G_{\text{TG}ji}$ terms is sufficiently large. For the case of the three considered toroidal phasing for heating and $R_{\text{Aeff}}=2\Omega/\text{m}$ we obtain for the generator powers $4.5 < P_{G+} < 5.9\text{MW}$ (without line losses).

Feedback control of the double stub tuners. The first stub St1 (antenna side) of the double stub tuner is positioned at V anti-node locations A...H. This stub can be replaced by an adjustable capacitor if we choose the corresponding double stub matching solution. The second stub St2 (at locations A'...H': see FIG. 4) is therefore inductive. For controlling the

capacitor C_{st1} and the stub $St2$ we use the measurement of the complex reflection coefficients $\Gamma_{A'...H'}$ at the stub $St2$ (generator side). Its real part controls the capacitor $St1$ and its imaginary part the inductive stub. The matching algorithm is therefore, e.g. for tuner 1: $\Delta C_{st1,A} \propto Re(\Gamma_{A'})$, $\Delta(l/\lambda_0)_{st2} \propto Im(\Gamma_{A'})$ where l is the stub length and λ_0 the wavelength.

FIG. 9 shows the obtained dynamics of the decouplers and reflection coefficients at hybrid outputs (Hyb) as a function of the number of control steps for simultaneous control of decouplers and double stubs tuners in the case of CD phasing (case of FIG. 5).

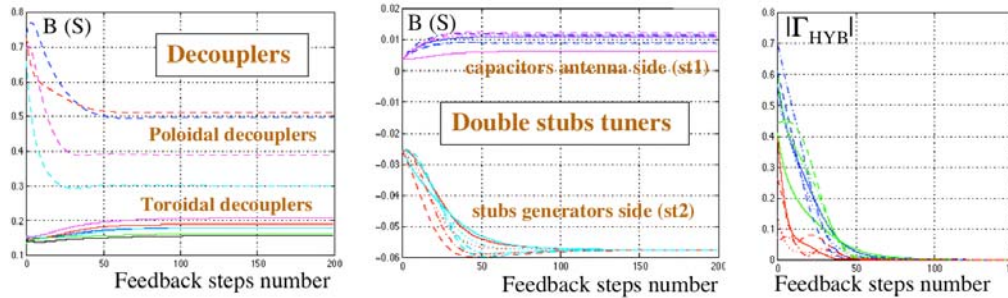


FIG. 9. Susceptance of the decoupler capacitors, the double stubs tuners versus their feedback step number. The resulting reflection coefficient at hybrids output is also shown.

5. Concluding discussion

The key features of the study are (i) the ability of decouplers to neutralize the adverse effects of mutual coupling for hybrid as for CT matching networks, (ii) the precise control of the antenna wave spectrum by the anti-node voltage distribution at the output of the antenna plug and particularly (iii) the use of the decouplers to feedback control these anti-node voltages. This results in a very effective matching solution for the network based on 3dB hybrids valid for heating as for current drive phasing with simultaneous feedback of the decouplers and compact tuners of the double stub type. The matching algorithms are robust and do not require RF measurements inside the antenna plug. Another way to handle the poloidal mutual coupling by the use of asymmetric hybrid couplers is proposed in ref. [13]. The CT option only requires 4 long lines, it maintains the total radiated power in the load resilience domain but loses its resilience if the strap inductance changes too much during the ELMs. It requires a more complicated matching procedure and is presently considered as a back-up solution.

References

- [1] P. Dumortier et al. Contract FU05-CT 2002-00094 (EFDA/02-675), Final Report (15 June 2003); Proc 15th Conf. RF Power in Plasmas (Moran 2003), p.94.
- [2] J. Jacquinet et al., Proc 17th Conf. RF Power in Plasmas (Clearwater 2007), p.13.
- [3] M. Nightingale et al., 22nd IAEA Fusion Energy Conference (2008).
- [4] A. Messiaen et al., Nucl. Fusion, 46(2006)S514.
- [5] P.U. Lamalle et al., Nucl. Fusion, 46(2006)432.
- [6] A. Messiaen et al., Fusion Engineering and Design, 74(2005)367.
- [7] M. Vervier et al., Proc 16th Conf. RF Power in Plasmas (Park City 2005), p.202.
- [8] P. Dumortier et al., Fusion Engineering and Design, 82(2007)758.
- [9] P. Dumortier et al., SOFT 2008, to be published in Fusion Engineering and Design.
- [10] P.U. Lamalle et al., Contract FU06-CT-2005-00187 (EFDA/05-1334), final report (July 2007), LPP-ERM/KMS lab. Report n° 130 (July 2007).
- [11] A. Messiaen et al., Proc 17th Conf. RF Power in Plasmas (Clearwater 2007), p.163.
- [12] P.U. Lamalle et al., Proc 17th Conf. RF Power in Plasmas (Clearwater 2007), p.139.
- [13] D. Swain et al., Final report on ITER TA No. G51TD15FU, November 2007.